JOC The Journal of Organic Chemistry

Article

pubs.acs.org/joc

Flash Flow Pyrolysis: Mimicking Flash Vacuum Pyrolysis in a High-Temperature/High-Pressure Liquid-Phase Microreactor Environment

David Cantillo, Hassan Sheibani,† and C. Oliver Kappe*

Christian Doppler Laboratory for Microwave Chemistry (CDLMC) and Institute of Chemistry, Karl-Franzens-University Graz, Heinrichstrasse 28, A-8010 Graz, Austria

Supporting Information

ABSTRACT: Flash vacuum pyrolysis (FVP) is a gas-phase continuous-flow technique where a substrate is sublimed through a hot quartz tube under high vacuum at temperatures of 400−1100 °C. Thermal activation occurs mainly by molecule−wall collisions with contact times in the region of milliseconds. As a preparative method, FVP is used mainly to induce intramolecular high-temperature transformations leading to products that cannot easily be obtained by other methods. It is demonstrated herein that liquid-phase high-temperature/high-pressure (high-T/p) microreactor conditions (160−350 °C, 90−180 bar) employing near- or supercritical fluids as reaction media can mimic the results obtained using preparative gas-phase FVP protocols. The high-T/p liquid-phase "flash flow pyrolysis" (FFP) technique was applied to the thermolysis of Meldrum's acid derivatives, pyrrole-2,3-diones, and pyrrole-2-carboxylic esters, producing the expected target heterocycles in high yields with residence times between 10 s and 10 min. The exact control over flow rate (and thus residence time) using the liquid-phase FFP method allows a tuning of reaction selectivities not easily achievable using FVP. Since the solution-phase FFP method does not require the substrate to be volatile any more —a major limitation in classical FVP—the transformations become readily scalable, allowing higher productivities and space−time yields compared with gas-phase protocols. Differential scanning calorimetry measurements and extensive DFT calculations provided essential information on pyrolysis energy barriers and the involved reaction mechanisms. A correlation between computed activation energies and experimental gas-phase FVP (molecule−wall collisions) and liquid-phase FFP (molecule−molecule collisions) pyrolysis temperatures was derived.

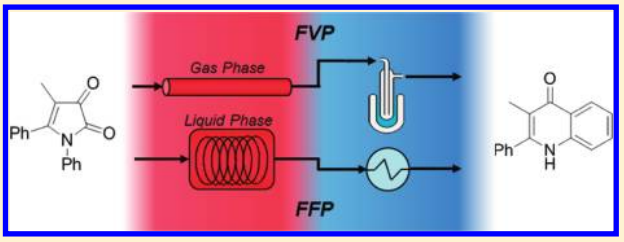

INTRODUCTION

Flash vacuum pyrolysis (FVP) is a special form of gas-phase thermolysis where a substrate is sublimed in vacuum through a quartz tube heated to temperatures of typically 400−1100 °C.[1−3] Using a sufficiently high vacuum (<10^{-3} mbar), thermal excitation of the molecules occurs mainly by molecule−wall collisions with mean residence times in the heated zone between 10^{-3} and 1 s.[2] The main advantage of the low-pressure FVP technique is the avoidance of intermolecular secondary reactions in the heated zone. It is, therefore, mainly used to induce high-temperature intramolecular transformations, such as eliminations, rearrangements, and cyclization processes.[1−3] Immediately after passage through the hot zone, the thermolyzate is typically cooled to very low temperatures (e.g., −196 °C) and thus protected from subsequent transformations.[1−3] Such "trapping" procedures allow the isolation and/or spectroscopic characterization of even highly reactive intermediates or reaction products.[4] Importantly, however, FVP conditions are also used as a valuable synthetic tool for the preparation of many interesting stable compound classes, in particular, unusual hetero- or carbocyclic systems that are sometimes difficult to prepare by other means.[1−3] The formation of these ring systems generally involves the initial formation of a reactive intermediate possessing a suitably disposed trapping group for intramolecular cyclization. Here, the FVP method is particularly useful for those cases where product formation under classical conditions is unfeasible because of extreme activation barriers that cannot be overcome at temperatures attainable by conventional (solution-phase) thermolysis techniques.[1−3]Although synthetic protocols involving FVP conditions possess many undisputed advantages, and—since performed in the absence of solvents and reagents—are generally considered as clean and efficient, several serious limitations do exist. Apart from the almost exclusive restriction to intramolecular transformations,[5] a major restraint is that the substrate generally must be volatile at reduced pressure; poorly volatile precursors are likely to decompose in the condensed phase upon heating prior to sublimation.[6] In addition, FVP protocols may be difficult to translate from laboratory (mg or g) to production (kg or t) scale in a reasonable time frame if the precursor is of only modest volatility.[3]

Unrelated to the popularity of preparative gas-phase FVP techniques throughout the past four decades,[1−3] the use of continuous-flow/microreaction technology for executing solution-phase organic synthesis has experienced significant growth in the past few years.[7−10] Enhanced heat and mass

Received: January 21, 2012
Published: February 9, 2012

transfer characteristics in the microstructured devices and the ability to accurately control reaction time by careful adjustment of residence times within microreactor units are the main advantages of this enabling technology.[8,9] An additional attractive feature of microreaction technology is the ease with which reaction conditions can be scaled through the operation of multiple systems in parallel (numbering-up, scaling-out), thereby readily achieving production-scale capabilities.[9] While traditionally, most synthetic transformations performed in microreactors have involved ambient or even low-temperature conditions in order to safely conduct highly exothermic and fast processes,[8,9] a more recent trend is to execute inherently slow synthetic transformations at elevated temperature conditions using sealed/pressurized continuous-flow devices in so-called high-temperature/high-pressure (high-T/p) process windows.[10] Similar to the use of batch microwave technology,[11] reaction times under these conditions can often be reduced from several hours to a few minutes. Importantly, using appropriate high-T/p flow instrumentation, many solvent systems can be utilized in their near- or supercritical (sc) state.[10] Supercritical fluids exhibit several distinct characteristics resulting from drastic changes in their physicochemical properties compared to standard conditions,[12] and continuous-flow organic synthesis in a variety of supercritical fluids, including CO_2, H_2O, and several organic solvents, has been reported in the literature.[12,13] When using organic solvents in their supercritical state under continuous-flow conditions, improved mass transfer due to the high diffusivity and improved hydrodynamic properties due to the very low viscosity of the reaction system can be expected.[13]

It can be argued that gas-phase FVP technology and solution-phase continuous-flow processing under high-T/p conditions are based on the same principle: the substrate, in gas or solution phase, respectively, is flowed through a hot reactor zone were the transformation takes place. Subsequently, the reaction mixture is cooled and the product or products are isolated. Therefore, it appeared to us that preparative transformations leading to a stable product typically performed under FVP conditions can alternatively be carried out in a continuous-flow reactor in a high-T/p reaction environment, without some of the restrictions of the traditional FVP protocol. Specifically, owing to the longer residence times in the solution-phase protocol, the required reaction temperatures should be considerably lower compared with those of the FVP method, reducing possible degradation phenomena of sensitive functional groups.[3] In addition, the solution-phase method does not require the substrate to be volatile any more, a major limitation in classical FVP. In the gas-phase FVP method, the residence time and other key experimental parameters are often difficult to monitor and control,[5] whereas the solution-phase microreactor method permits a much better control of reactor temperature, flow rate, and residence time, allowing a fine-tuning of reaction selectivity.[8,9]

Herein, we demonstrate that high-T/p continuous-flow conditions employing near- or supercritical (sc) fluids as reaction media can mimic the results obtained using more traditional gas-phase FVP protocols. Several previously studied FVP transformations involving reactive ketene intermediates were used as examples to evaluate the efficiency and robustness of this novel pyrolytic technique, termed flash flow pyrolysis (FFP). Gratifyingly, operating in a temperature range of 160−350 °C with residence times of a few seconds or minutes, most target heterocycles could be obtained in high yields and excellent purities after a simple workup, often surpassing the results achievable with FVP or other enabling technologies, such as microwave chemistry. Differential scanning calorimetry (DSC) measurements in combination with DFT calculations were employed to support the mechanistic and kinetic investigations.

RESULTS AND DISCUSSION

General Considerations. The continuous-flow chemistry described in this work was carried out in a commercial high-T/p microtubular flow unit that can be used for processing homogeneous reaction mixtures (ThalesNano X-Cube Flash).[14] The reactor uses stainless steel coils (i.d. 1000 μm) of variable length (4, 8, and 16 mL volume) that can be directly heated across their full length by electric resistance heating to temperatures up to 350 °C. The reaction mixture is introduced to the reactor block containing the steel coils and a heat exchanger via one (or more) standard HPLC pump. The system pressure valve sets and stabilizes the set pressure value between a pressure range of 50 and 180 bar.[14] For experiments in a more moderate temperature range (150 °C), a Uniqsis FlowSyn reactor was also used in a few instances.

For our initial optimization studies, microwave batch technology using a high-field density single-mode microwave reactor (Anton Paar Monowave 300) allowing accurate internal temperature monitoring was employed (maximum operating conditions: 300 °C/30 bar).[15] Recent work has demonstrated that FVP reaction conditions can be simulated to some extent by the rapid heating and high temperatures characteristic of microwave-assisted processes.[16−18] Conversely, batch microwave chemistry has been successfully translated to conventionally heated continuous-flow processes under high-T/p conditions ("microwave-to-flow" paradigm).[19] In this context, a significant advantage of flow instrumentation using stainless steel reactor coils is that typically much harsher reaction conditions compared with standard microwave instruments employing sealed Pyrex vials can be employed. Specifically, the utilization of these flow devices allows the use of higher system pressures, and thus the application of low-boiling solvents in their supercritical state.[10] Given these premises, the suggested adaptation of FVP conditions to liquid-phase high-T/p flow chemistry appeared feasible.

As suitable model reactions for our investigations, we have selected a number of classical FVP transformations that involve ketenes as reactive intermediates, which subsequently undergo either internal trapping via cyclization or dimerization processes. Ketene derivatives are common intermediates in many FVP reactions and are typically generated by a clean thermal decomposition of suitable precursor molecules, including thermolabile heterocycles, diazoketones (Wolff rearrangement), or carboxylic acid derivatives.[20,21] Specifically, we have chosen the pyrolysis of benzoyl-Meldrum's acid **1a**, acylamino-methylene-Meldrum's acid **2**, pyrrole-2,3-dione **3**, and methyl pyrrole-2-carboxylate (**4**) as model reactions. All transformations have been previously studied under analytical and preparative FVP conditions, and the individual reaction pathways leading to the corresponding stable heterocycles are generally well-understood. To investigate some of these transformations in more detail, differential scanning calorimetry (DSC)[22,23] measurements of substrates and products were performed. In addition, DFT calculations were carried out in those instances where unusual reactivities were observed in the pyrolysis processes and to obtain information on the involved pyrolysis energy barriers.

dx.doi.org/10.1021/jo3001645 | J. Org. Chem. 2012, 77, 2463−2473

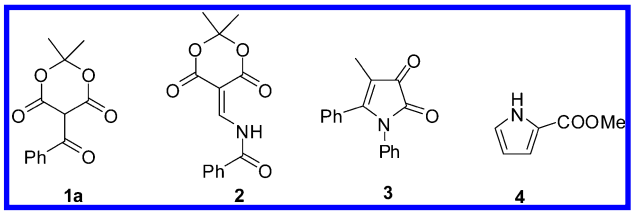

Pyrolysis of Acyl Meldrum's Acid Derivative 1a. The thermal chemistry of Meldrum's acid derivatives has been widely investigated since the 1970s by several research groups.[24] At elevated temperatures, Meldrum's acid analogues generally lose CO_2 and acetone in a concerted fashion, thereby generating a ketene intermediate.[24] In the case of acyl Meldrum's acids, the resulting α-oxoketene intermediate can be trapped by various reactive functionalities to provide a number of useful products.[25] Thus, the reaction with imines[26] gives rise to 1,3-oxazine-4-ones, β-lactams, and 2-pyridones, whereas the addition of aldehydes,[17,27] nitriles,[28] alcohols,[29] and amides[30] results in dioxinones, 1,3-oxazin-4-ones, β-ketoesters, and *N*-acylacetylcarboxamides, respectively.

FVP studies on this type of Meldrum's acid have been mainly performed using acetyl Meldrum's acid (**1b**) as a precursor at temperatures ranging from 450 to 650 °C (10^{-5} bar), providing acetylketene **5b**, which has been isolated and characterized by low-temperature IR spectroscopy (Scheme 1).[31] In solution, in

Scheme 1

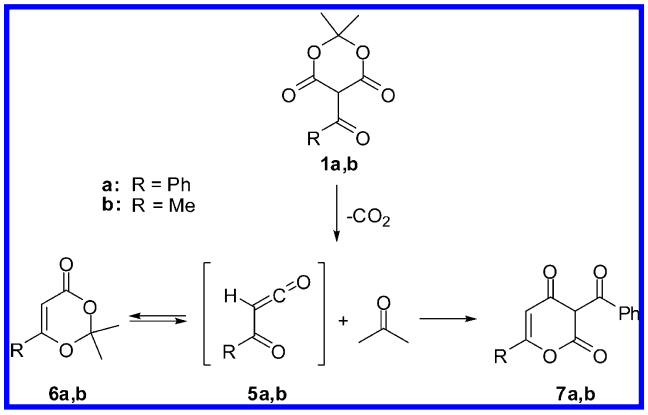

the absence of nucleophilic trapping reagents, the α-oxoketene intermediate reacts at moderate temperatures with the released acetone to form 1,3-dioxin-4-one **6b**, commonly known as "acylketene-acetone adduct", in itself a useful synthetic precursor for acetylketene.[17,32] 1,3-Dioxin-4-ones of type **6** are often stable at temperatures below 100 °C. When the temperature is further increased, the α-oxoketene [4 + 2] dimers **7** are formed in good yields and, even in the presence of nucleophiles, dimers **7** are often byproducts observed in reactions involving α-oxoketenes.[17,25,32,33]

For our studies on the high-T/p flow pyrolysis of acyl Meldrum's acid derivatives, we have selected the benzoyl derivative **1a**. As an initial screening method to determine the required decomposition temperature, we have performed several DSC measurements (Figure 1).[23] As can be seen from the DSC analysis, acyl Meldrum's acid **1a** melts at 105 °C, immediately followed by substrate decomposition (in agreement with literature data).[26a] At ca. 150 °C, a further decomposition event is seen, which, by comparison with the DSC data of pure **6a**, can be readily assigned to the decomposition of the initially formed 1,3-dioxin-4-one intermediate **6a**. The ultimate product

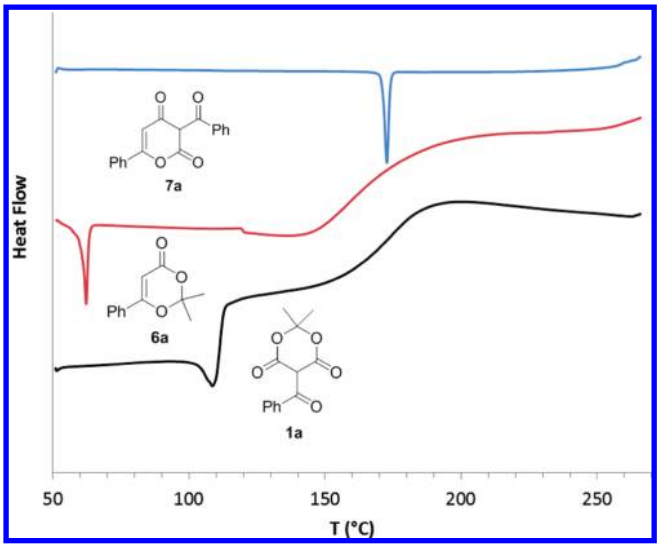

Figure 1. Differential scanning calorimetry (DSC) data of substrate **1a**, intermediate **6a**, and final product **7a** (Scheme 1).

of the neat decomposition of both **1a** and **6a** is α-oxoketene dimer **7a**, which is stable until 250 °C (mp 172–173 °C).

Of particular interest to us was to demonstrate that, using a liquid-phase high-T/p continuous-flow method with an exact residence time control, the thermal decomposition of benzoyl Meldrum's acid (**1a**) could be tuned to provide either the 1,3-dioxin-4-one intermediate **6a** or the oxoketene dimer **7a**. Taking the onset decomposition temperatures measured by DSC for **1a** (105 °C) and **6a** (~150 °C) as a reference, initial optimization experiments were performed using sealed-vessel microwave batch technology in 1,2-dimethoxyethane (DME). Having the optimized conditions in hand (see Tables S1 and S2 in the Supporting Information), the reactions were then translated to a high-T/p continuous-flow protocol. When a temperature of 100 °C (90 bar set pressure) was chosen, the decomposition of benzoyl Meldrum's acid **1a** (0.25 M in DME) required 2 min for completion (full consumption of starting material), providing a selectivity for the 1,3-dioxin-4-one **6a** of close to 90% (Table 1). When dimer **7a** is the preferred

Table 1. Selectivity in the Pyrolysis of 1a and 6a under Microwave Batch and Continuous-Flow Conditions

substrate	temperature (°C)/time (min)	HPLC yield[a] (%) **6a**[b]	HPLC yield[a] (%) **7a**[b]	isolated yield[b,c] (%)
1a	100/2	89/88	5/4	**6a** (67/65)
1a	200/1		98/95	**7a** (82/80)
6a	200/1		97/93	**7a** (77/78)

[a]Peak area integration at 215 nm, corrected for relative response factors. [b]Microwave batch/continuous flow. [c]After column chromatography.

product, the reaction proceeds to completion in 1 min at 200 °C (90 bar set pressure), with a very good selectivity of ~98%. Although full conversion was always obtained, small amounts (~5%) of unidentified byproducts were observed in most cases. To demonstrate the reversible character of the formation of **6a** from benzoylketene (**5a**)[34] and acetone, the pure isolated α-oxoketene–acetone adduct **6a** was also subjected to pyrolysis at the same conditions (Table 1). As expected, analogous results were obtained for both conversion and selectivity.

dx.doi.org/10.1021/jo3001645 | J. Org. Chem. 2012, 77, 2463–2473

It should be emphasized that the excellent selectivity seen in the generation of 1,3-dioxin-4-one intermediate **6a** can be ascribed to the exquisite control over the reaction time and temperature attainable in dedicated microwave batch and continuous-flow reactors. In particular, the very efficient heating and cooling in both reactor systems allows these high levels of selectivity to be obtained.

On the basis of the observations made above, it can be presumed that the formation of 1,3-dioxin-4-one **6a** from benzoylketene (**5a**) and acetone is a fast equilibrium process, whereas the α-oxoketene dimerization would be slower and irreversible (Scheme 1). This hypothesis was supported by a dissection of the reaction energetics through DFT calculations. Thus, the transition states for the formation of **6a** and **7a** from benzoylketene (**5a**) were calculated at the M06-2X/6-311G-(d,p) level[35] using the Gaussian 09 package.[36] Solvent effects were included through the SMD method.[37,38] Figure 2 depicts

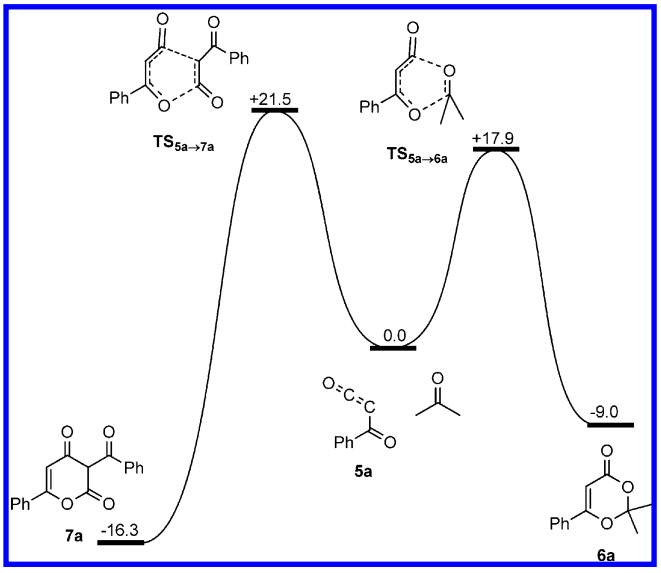

Figure 2. Relative free energy (kcal mol^{-1}) for the intermediates, transition structures, and products formed during the pyrolysis of the Meldrum's acid derivative **1a**.

the energy profile for the two competitive processes, using as reference the free energy of acetone and the ketene (**5a**) generated in the pyrolysis. As expected, the formation of 1,3-dioxin-4-one **6a** exhibits a lower barrier, and the relative free energy of the benzoylketene–acetone cycloadduct **6a** is lower than that of the benzoylketene intermediate by 9.0 kcal mol^{-1}, thus explaining why **6a** is rather stable at room temperature, and heat needs to be applied to generate the benzoyl ketene (**5a**). The formation of the benzoylketene dimer **7a** has a higher energy barrier, of +21.5 kcal mol^{-1}, which is, however, not enough to induce complete selectivity ($\Delta\Delta G^{\ddagger} \sim 3$ kcal mol^{-1}). This explains why, in all experimental studies, small amounts of the benzoylketene dimer**7a** were observed, even at a moderate temperature of 100 °C. Moreover, the dimerization can be considered as an irreversible process, because 16.3 kcal mol^{-1} is released during the transformation (Figure 2). Figure 3 shows the optimized geometry of the transition states leading to the benzoylketene–acetone adduct **6a** and the benzoylketenedimer **7a**.

In case of competitive reaction pathways showing these differences in activation energy, the most common way for tuning the selectivity is the control of temperature, as described above. However, as an alternative, the reaction (residence) time can be varied at a given temperature. To accomplish this goal experimentally, a rapid heating and cooling of the reaction mixture is required, thus ensuring accurate reaction times. Gratifyingly, both (small scale) microwave batch technology and continuous-flow microreactors provide the efficient heat transfer necessary for this purpose. A close inspection of the DSC data (Figure 1) reveals that, if the reaction would be performed at a temperature of ~150 °C, the formation of **6a** should be a very fast process, while dimer **7a** would be formed more slowly. Choosing 150 °C as set reaction temperature for the decomposition of benzoyl Meldrum's acid (**1a**) in DME, a series of experiments were performed where only the reaction/residence times (batch/flow) were varied (Figure 4). In all cases, full conversion of the substrate **1a** was observed. As expected, for short reaction times, the selectivity for the benzoylketene–acetone adduct (**6a**) was high, while as the reaction time increased, dimer **7a** was the favored product. It has to be emphasized that, for very short reaction times, the selectivities were somewhat higher in the flow reactor compared to the microwave batch experiment (85% versus 80% at 10 s). This can be rationalized by a better command over the exact residence time in the heated zone of the flow reactor compared to the achievable control over the reaction time in a microwave batch experiment, which typically involves significant heating (ramp) and cooling times not experienced in microreactors.[39] Under extreme conditions, complete conversion of the starting material **1a** at 150 °C in flow was observed after a residence time of only 7 s (corresponding to a flow rate of 20 mL/min and a reactor volume of 2.5 mL), providing a selectivity close to 90% for **6a**.[40]

Pyrolysis of Acylaminomethylene Meldrum's Acid Derivative 2. Aminomethylene Meldrum's acids of type **2** have been used as substrates for the preparation of 2-substituted-1,3-oxazin-6-ones **9** by either FVP at 500–550 °C[41] or static thermolysis either in decaline solution or neat at

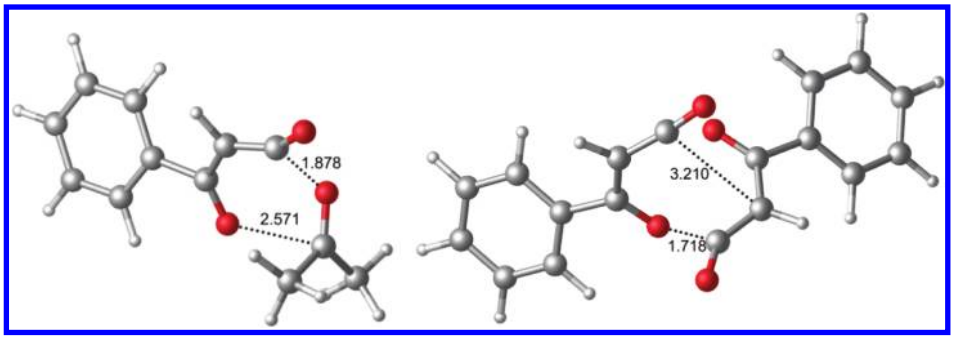

Figure 3. Optimized geometries for the transition states leading to adducts **6a** and **7a** (Figure 2).

dx.doi.org/10.1021/jo3001645 | J. Org. Chem. 2012, 77, 2463–2473

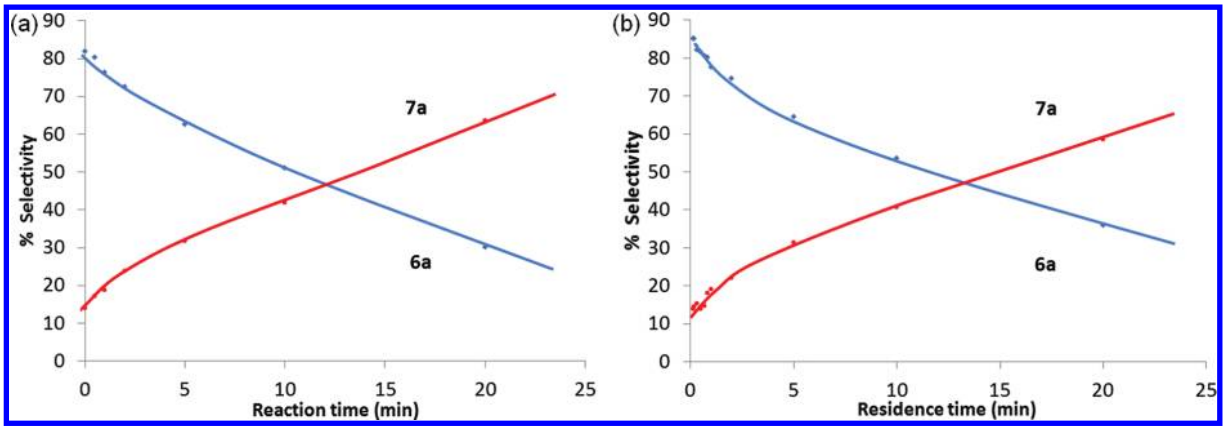

Figure 4. Selectivity in the pyrolysis of benzoyl Meldrum's acid (**1a**) at a 150 °C temperature as a function of (a) reaction time (microwave) and (b) residence time (flow).

165−185 °C.[42] The postulated mechanistic pathway for this transformation is shown in Scheme 2.[41,43] Pyrolysis of

Scheme 2

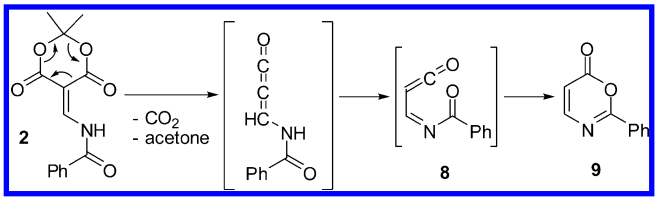

Meldrum's acid **2** releases acetone and CO_2 with concomitant formation of a methyleneketene, which, upon H-transfer, leads to an *N*-acylimidoylketene of type **8** that subsequently undergoes electrocyclization to the 1,3-oxazin-6-one **9** in the final step.[43]

DSC analysis of model substrate *N*-benzoylaminomethylene Meldrum's acid **2** again provided useful data about the expected decomposition temperature and product stability (Figure S1 in the Supporting Information). Since the decomposition of **2** was observed at ∼240 °C (with 1,3-oxazin-6-one **9** being stable up to a temperature of ∼290 °C), this temperature region was used as a reference point for our initial optimization studies.

The most significant results for the pyrolysis of Meldrum's acid derivative **2** in toluene (0.25 M) under both microwave batch and continuous-flow conditions are summarized in Table 2. In all cases, the data correspond to the reaction or

Table 2. Isolated Product Yields of 1,3-Oxazin-6-one 9 in the Pyrolysis of 2 in Toluene under Microwave Batch and Continuous-Flow Conditions (Scheme 2)

heating mode	temperature (°C)	time (min)	yield (%)[a]
MW	240	5	88
MW	250	2	90
flow	250	2	87
flow	260	1	85
flow	270	0.5	88

[a]The HPLC conversion in all cases was >99%.

residence times necessary to obtain full conversion at a given temperature. When the experiments were performed under microwave conditions at 250 °C, the reaction proceeded to completion within 2 min (see Table 3 in the Supporting Information). A further increase of the reaction temperature was not possible due to the high autogenic pressure generated by the solvent (>30 bar) at these temperatures, exceeding the maximum pressure limit of the microwave instrument. Pyrolysis in flow conditions reproduced the microwave batch results, leading to very similar conversions and isolated product yields when identical temperature/time profiles were employed. The significantly wider operational limit of the flow instrument allowed us to perform the pyrolysis also at higher temperatures (Table 2). Thus, an increase of the temperature in the reactor zone to 270 °C resulted in a very rapid pyrolysis reaction, with a residence time of only 30 s at a flow rate of 8 mL/min (reactor volume 4 mL).

It is worth to point out the significant difference in reactivity between Meldrum's acid derivatives **1a** and **2**. To achieve fast thermolysis of the substrates, temperatures of approximately 160 and 270 °C are required for **1** and **2**, respectively, which accounts for the higher stability of the acylaminomethylene Meldrum's acid derivative **2**. M06-2X/6-311G(d,p) calculations of the energy barriers revealed equivalent mechanisms for the pyrolyses of **1** and **2**, which both consist of a concerted extrusion of CO_2 and acetone from the substrate. At this level of theory, the barriers for the pyrolyses are 35.2 and 40.9 kcal mol^{-1} for **1** and **2**, respectively. An estimation of the rate constants through the Eyring equation shows that longer reaction times, even hours, or, alternatively, higher temperatures should be required for completion with such barriers. The energy barriers at this level appear to be overestimated by approximately 5−6 kcal mol^{-1}, but, however, are sufficient to qualitatively explain the greater stability of **2**, with an energy barrier for the decomposition ∼5 kcal mol^{-1} higher with respect to **1a**. Figure 5 shows the optimized geometries for both transition states.

Pyrolysis of Pyrrole-2,3-dione 3. The thermal decomposition of 1-phenyl-2,3-dihydropyrrole-2,3-diones via FVP or solution-phase thermolysis generates highly reactive imidoylketenes that subsequently cyclize to 4-quinolones (Scheme 3).[44] Specifically, the formation of quinolone **11** from pyrroledione **3** has been described using either FVP at 700 °C/10^{-4} mbar[44a] or diphenylether as solvent at 280 °C (10 min).[16] In general, the FVP of pyrroledione precursors (cheletropic extrusion of CO) requires significantly higher temperatures compared with the thermolysis of the corresponding Meldrum's acid derivatives (concerted extrusion of CO_2 and acetone) to generate the corresponding imidoylketenes.[44] For example, whereas the pyrolysis of pyrroledione **3** is carried out at 700 °C,[44a] Meldrum's acid **2** only requires 500−550 °C to be fully thermolyzed in the gas

dx.doi.org/10.1021/jo3001645 | J. Org. Chem. 2012, 77, 2463−2473

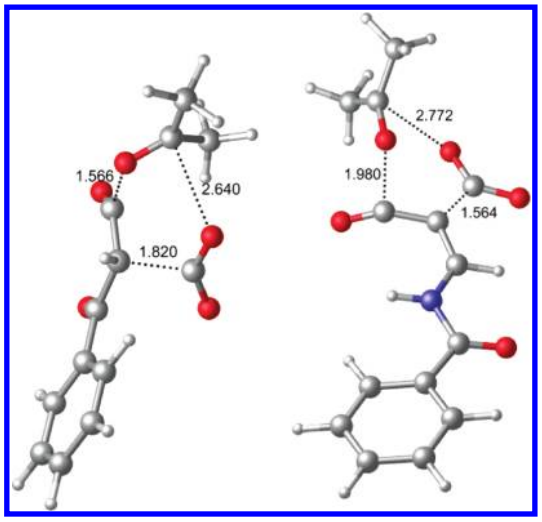

Figure 5. Optimized geometries (M06-2X/6-311G(d,p) level) for the transition states corresponding to the thermolysis of the Meldrum's acid derivatives **1a** (left) and **2** (right).

Scheme 3

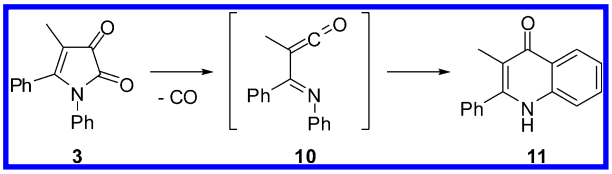

phase.[41] This difference is also reflected in the required solution phase[41,43]and neat[45] thermolysis experiments, the latter revealing a CO extrusion at temperatures above 300 °C.

In an attempt to translate the gas-phase FVP of pyrroledione **3** to a corresponding liquid-phase high-T/p flow protocol, we initially screened a variety of solvents under microwave batch conditions, keeping the general requirement for reaction homogeneity in continuous-flow chemistry in mind.[8,9] At a 300 °C reaction temperature, full conversion was achieved within 20 min in a number of solvents, including toluene, chlorobenzene, and anisole (see Table S4 in the Supporting Information). This relatively long solution-phase reaction time at 300 °C is in agreement with the visually observed neat thermolysis temperature.[45] Operating at these temperatures in a microwave batch reactor with a pressure limit of 30 bar severely restricted the solvent selection, essentially excluding solvents with boiling points lower than 100 °C. When the flow reactor with a pressure limit of 180 bar is used, this limitation does not exist.[14,39,46] We have, therefore, selected acetonitrile as the solvent for the high-T/p liquid-phase pyrolysis of pyrroledione **3**, which solubilizes both the starting material and the product very well. The flow pyrolysis of pyrroledione **3** in acetonitrile (0.1 M) was performed in a temperature range of 310–340 °C (130 bar set pressure) (see Figure S2 in the Supporting Information). It should be emphasized that, at these operating conditions, acetonitrile becomes a supercritical fluid (T_c, 272 °C; P_c, 48.7 bar) exhibiting very low viscosity and high diffusivity.[12,13] The flow pyrolysis of pyrroledione **3** in scMeCN at 340 °C was remarkably clean and proceeded without any byproducts in a residence time of only 15 s (16 mL min^{-1} flow rate; reactor volume, 4 mL).[47] Since no side reactions occurred (see Figure S3 in the Supporting Information for an HPLC trace), workup simply consisted of evaporation of the solvent under reduced pressure, providing quinolone **11** in quantitative yield. Continuous pyrolysis of the liquid stream for 1 h would thus lead to 23 g of product, a considerably higher productivity and space–time yield than that achievable through a classical FVP approach limited by substrate volatility.

Mechanistically, when pyrroledione **3** is heated, it releases a CO molecule in a cheletropic 4 + 1 cycloreversion with an energy barrier of +45.2 kcal mol^{-1}, leading to imidoylketene **10** (Figures 6 and 7). Subsequent ring closure occurs through

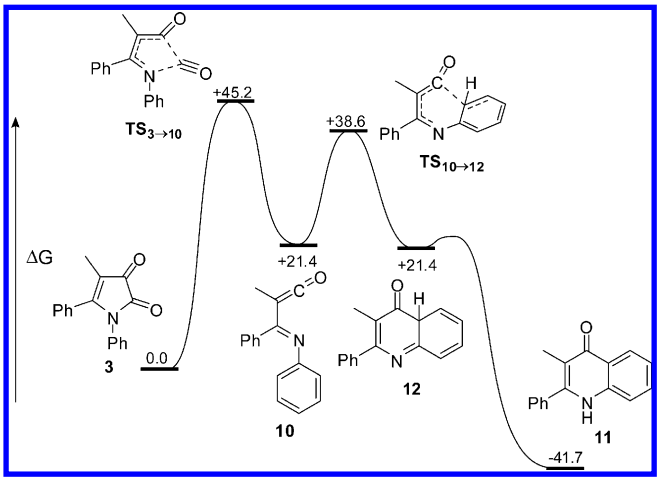

Figure 6. Relative free energy (kcal mol^{-1}) of the stationary points involved in the formation of quinolone **11** from the pyrolysis of **3** calculated at the M06-2X/6-311G(d,p) level.

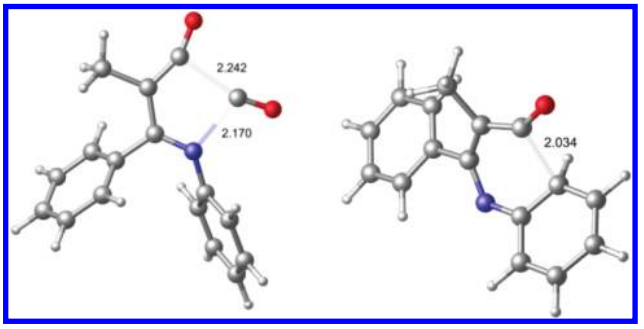

Figure 7. Optimized transition structures for the formation of **10** and **12** (Figure 6).

nucleophilic attack of the electron-rich aromatic ring onto the ketene carbon. Interestingly, this electrophilic aromatic substitution takes place through a barrier of only 17.2 kcal mol^{-1} with respect to the intermediate **10**, 38.6 kcal mol^{-1} with respect to the starting material (**3**). Thus, the key step in the overall process obviously is the formation of imidoylketene **10** from the pyrolysis of the pyrroledione **3**, followed by an efficient generation of the quinolone moiety (**11**). The significant theoretical barrier for the process (+45.6 kcal mol^{-1}) explains the drastic conditions (>300 °C) necessary for carrying out this reaction in solution phase. Similar calculations on the cyclization of imidoylketenes have been previously reported at the B3LYP/6-31G(d) level of theory, also revealing low energy barriers for the electrocyclization process leading to the quinolone moiety.[48]

Pyrolysis of Methyl Pyrrole-2-carboxylate (4). To further benchmark our liquid-phase flow pyrolysis approach, we subsequently evaluated a more difficult transformation: the pyrolysis of methyl pyrrole-2-carboxylate (**4**). This reaction is

dx.doi.org/10.1021/jo3001645 | J. Org. Chem. 2012, 77, 2463–2473

known to initially generate the five-membered ring ketene (azafulvenone) intermediate **13**, which subsequently dimerizes to 2,5-diketopiperazine **14** (pyrocoll) (Scheme 4).[49] Under FVP

Scheme 4

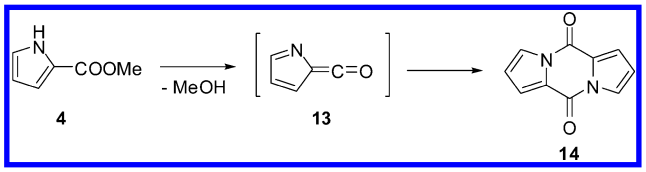

conditions, this elimination of MeOH requires 700−850 °C to obtain **14** in 90% yield (the remainder being starting material).[49] If the reaction is performed at lower temperatures, the conversion decreases dramatically (FVP at 750 °C furnished only 62% of **14**).[49] Solution-phase thermolysis protocols of pyrrole-2-carboylic acid or its esters to provide 2,5-diketopiperazine **14** have not been described in the literature,[50] and our own experiments heating pyrrole-2-carboylic acid or its methyl ester (**4**) in DMF at 220 °C for 30 min did not provide any isolable quantities of pyrocoll (**14**).

Similar to the pyrroledione pyrolysis described above, we have chosen scMeCN as a reaction environment for the flow pyrolysis of pyrrole-2-carboylate **4**. At temperatures ranging from 320 to 350 °C (130 bar), complete consumption of the starting material with concomitant formation of pyrocoll (**14**) was achieved within residence times of 5−7 min. It should be noted that the formation of pyrocoll (**14**) by thermolysis of a pyrrole-2-carboylate in the absence of any catalyst or reagent has so far only been reported by FVP conditions at high temperatures (700−850 °C). This, in a way, highlights the similarity of liquid-phase continuous-flow chemistry under high-T/p conditions and the FVP approach.

On the other hand, we have found that the liquid-phase method led to the formation of significant amounts of pyrrole (**16**) as a byproduct, apparently not seen in the gas-phase FVP procedure.[49] In the flash flow pyrolysis, the pyrrole/pyrocoll (**16**/**14**) ratio was affected by the concentration of the reaction mixture. Thus, whereas a 0.05 M solution of pyrrole-2-carboxylate **4** when pyrolyzed at 330 °C for 5 min favored the formation of pyrrole (71:29 **16**/**14** HPLC ratio), a more concentrated solution (0.1 M) processed under otherwise identical conditions produced more pyrocoll (46:54 **16**/**14** HPLC ratio). The selectivity for pyrocoll (**14**) was ultimately optimized to 59%, pyrolyzing a 0.2 M solution of pyrrole-2-carboylate **4** at 330 °C (7 min), providing a 55% isolated yield of pyrocoll (**14**). The formation of pyrrole (**16**) can be rationalized through the decarboxylation of the ester substrate **4**. This unusual and surprising ester decarboxylation is likely to follow a Krapcho decarboxylation-type mechanism,[51] in which the methanol released during the initial elimination step (**4** → **16** + MeOH) plays the role of the nucleophile (Scheme 5). Thus, the

Scheme 5

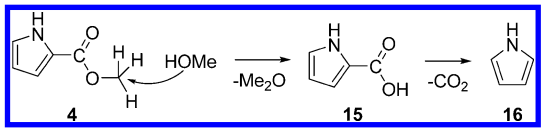

OH group in methanol attacks the methyl ester in **4**, leading to dimethylether and pyrrole-2-carboxylic acid (**15**), which readily releases CO_2 at the operating temperatures. With the purpose of demonstrating the key role of methanol for this proposed mechanism, the pyrolysis reaction was additionally carried out using a 1 M solution of methanol in acetonitrile as solvent. In the presence of the methanol additive, the ratio of pyrrole/pyrocoll increased to ∼2:1, and interestingly, half of the starting material **4** (51%) remained unchanged. This low conversion can be accounted for by an equilibrium between the methyl pyrrole-2-carboxylate (**4**) and the resulting pyrolyzate (azafulvenone **13** + MeOH), which favors the starting material when methanol is added to the reaction mixture.

The formation of the azafulvenone intermediate **13** and the unexpected ester decarboxylation leading to pyrrole (**16**) are, therefore, competing pathways under the reaction conditions. To shed light into the reactivity, calculations of the energy barriers for the competing mechanisms were performed at the M06-2X/6-311G(d,p) level, including the solvent effect (acetonitrile, SMD method) (Figure 8). The release of

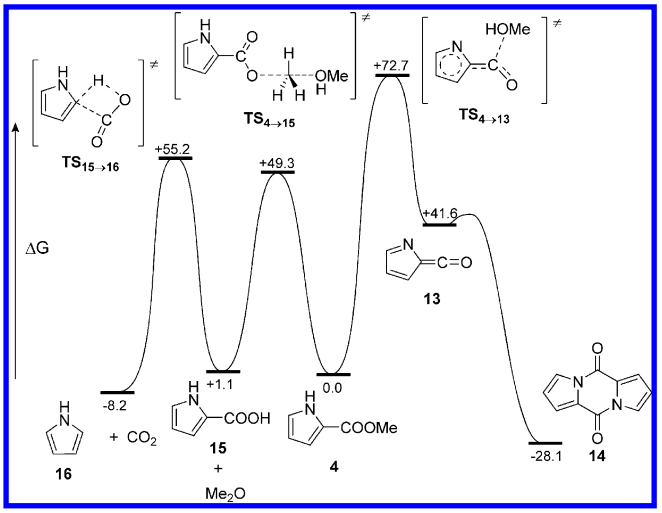

Figure 8. Energy profile (kcal mol^{-1}) (M06-2X/6-311G(d,p) level) for the competitive processes involved in the pyrolysis of methyl pyrrole-2-carboylate (**4**).

methanol from the starting material (**4**) implies an initial transfer of the relatively acidic nitrogen proton from the pyrrole moiety to the carbonyl group and the subsequent cleavage of the C−O bond. The overall energy barrier for the process is more than 72 kcal mol^{-1}, very high in comparison with the previously calculated barriers for the degradation of the Meldrum's acid derivatives (**1a** and **2**) and the pyrrole-2,3-dione **3**. This explains that, even at 330−350 °C, the transformation requires several minutes for completion. The methanol molecule released during the formation of the azafulvenone intermediate **13** can then react with ester **4** through the above-mentioned Krapcho decarboxylation mechanism. In a first step, the nucleophilic methanol attacks the methyl ester, giving rise to pyrrole-2-carboxylic acid (**15**) and dimethyl ether. This process takes place through an energy barrier of 49.3 kcal mol^{-1} (Figure 8), very low in comparison with the formation of the ketene. The pyrrole-2-carboxylic acid then undergoes decarboxylation with release of CO_2. The corresponding energy barrier, 55.2 kcal mol^{-1}, is higher than that for the previous nucleophilic substitution, but still much lower than that required for pyrolysis. These energetics explain the high amounts of pyrrole detected in the pyrolyzate after the flow reaction. Because the formation of

dx.doi.org/10.1021/jo3001645 | J. Org. Chem. 2012, 77, 2463−2473

pyrrole is faster, the methanol molecules released during the pyrolysis rapidly react with the remaining substrate **4** in solution, leading to pyrrole (**16**). Under gas-phase FVP conditions, the possibility for the intermolecular pathway **4** + MeOH → **16** + Me_2O is severely restricted, which highlights one of the main advantages of the FVP technique compared to classical thermolysis protocols in solution.[1−3,5]

Pyrolysis of Azulene to Naphthalene. As a final example, we have attempted the azulene-to-naphthalene rearrangement (Scheme 6),[52] which, although preparatively useless, has been

Scheme 6

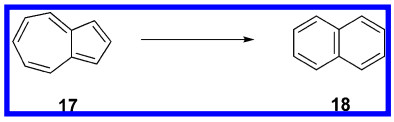

studied extensively from the mechanistic point of view, both experimentally[53] and theoretically.[54−56] Under gas-phase FVP conditions, the thermal isomerization requires temperatures of ∼1100 °C to achieve good conversions,[53d] while static pyrolysis at 330 °C takes 48 h to reach completion.[52,57] In our experiments, using high-T/p continuous-flow conditions, a solution of azulene (**17**) (0.1 M) was processed at 350 °C in scMeCN for several min (5−10 residence time). Disappointingly, not even trace amounts of naphthalene (**18**) were detected in the reaction mixture by GC analysis. Although a full optimization using different solvents was not performed, it is clear that a liquid-phase approach involving a solvent will be extremely challenging since the decomposition of the solvent at higher temperatures (400−500 °C) must clearly be taken into account.

The energy barrier for this rearrangement must, therefore, be considerably higher compared with that of the other pyrolysis reactions discussed herein (see above). The most plausible mechanisms for the azulene-to-naphthalene rearrangement have been suggested to be the "spiran pathway" or the "methylene walk".[55] Our theoretical calculations at the M06-2X/6-311G-(d,p) level for the corresponding key transition states reveal energy barriers above 100 kcal mol^{-1} for both mechanistic proposals, in either gas phase or acetonitrile solution (see Table S5 in the Supporting Information), thus explaining the more than drastic conditions necessary to perform the rearrangement.

■ CONCLUSIONS

In summary, we have demonstrated that liquid-phase continuous-flow processing in a high-temperature/high-pressure (high-T/p) regime is a useful synthetic method to perform pyrolysis reactions that are typically carried out using flash vacuum pyrolysis (FVP) protocols. Although it appears counterintuitive that chemistry that is performed under high vacuum (10^{-3} mbar) in the gas phase can be mimicked by a high-pressure (>100 bar) liquid-phase method, the results presented herein demonstrate that similar results can be obtained for most cases using flash flow pyrolysis (FFP) and FVP. This is particularly true for those instances where stable products derived from intramolecular reaction pathways are formed. However, as the examples discussed herein demonstrate, also in the case of dimerization reactions, the liquid-phase results are generally comparable to the outcome of FVP experiments.

The main advantage of the liquid-phase high-T/p continuous-flow protocol is the significantly better control over the residence time in the heated zone, often allowing the fine-tuning of selectivity to a level not possible under FVP conditions. In addition, liquid-phase flow protocols can be readily scaled to production volumes, something that is not easily achieved in preparative FVP, in particular, for nonvolatile starting materials. Clearly, one of the main characteristics of the low-pressure gas-phase FVP method is the avoidance of intermolecular secondary reactions in the heated zone. This feature is difficult to duplicate in liquid phase, and it has to be noted that the solvents and reactor materials used for these microreactor transformations must generally be inert and anhydrous, at least for the examples studied herein, where reactive species (i.e., ketenes) are generated as transient intermediates, or the substrates themselves are sensitive to moisture. We have also shown that, in some extreme cases, the maximum reaction temperatures attainable in standard liquid-phase flow reactors (350 °C) are not high enough to induce a pyrolysis reaction. For those cases, FVP remains the method of choice.

Throughout our investigations, we have heavily relied on DFT calculations at the M06-2X level as a valuable tool for explaining and/or predicting the energetic requirements and the plausibility for a specific pyrolytic process or observed selectivity. Although, at this level of theory, the energy barriers appear to be overestimated, a comparison between the individual processes allows a qualitative estimation of the energetic requirements and, therefore, a rough guide for reaction temperatures to be used in FVP and liquid-phase FFP protocols (Table 3). As the contact (residence) times in FVP are extremely short and thermal excitation of the molecules occurs mainly by molecule−wall collisions, the required reaction temperatures (furnace temperature) are significantly higher compared to the liquid-phase approach (molecule−molecule collisions). Estimation of the rate constants through the Eyring equation allows a rough assessment of the theoretical completion times for the pyrolyses. As described above, in the case of the Meldrum's acid derivatives, the barrier seems to be overestimated by 5−6 kcal/mol, thus leading to higher theoretical completion times than encountered experimentally. For the pyrroledione **3**, the barrier is overestimated by ca. 4 kcal mol^{-1}, and the predicted completion time is several minutes instead of a few seconds. However, although the theoretical level employed cannot quantitatively predict

Table 3. Theoretical Energy Barriers (M06-2X/6-311G(d,p) Level) for the Pyrolyses of the Different Substrates and Experimental Conditions Required for Liquid-Phase (FFP) and FVP Pyrolysis

substrate	calculated energy barrier (kcal mol^{-1})	reaction temp (°C) (FVP)	reaction conditions liquid phase
Meldrum's acid **1b**	∼35	∼400[a]	160 °C, 10 s
Meldrum's acid **2**	∼40	∼550[b]	270 °C, 15−30 s
pyrroledione **3**	∼50	∼700[c]	340 °C, 15−30 s
pyrrole-2-carboxylate **4**	∼70	∼850[d]	330−350 °C, 5−10 min
azulene **17**	∼100	1000−1100[e]	

[a]Reference 31a. [b]Reference 41b. [c]Reference 44a. [d]Reference 49. [e]Reference 53d.

dx.doi.org/10.1021/jo3001645 | J. Org. Chem. 2012, 77, 2463−2473

accurate barriers or reaction times, is a valuable tool to qualitatively assess feasibility of these pyrolytic processes.

EXPERIMENTAL SECTION

Computational Details. All of the calculations reported in this work were carried out using the Gaussian 09 package.[36] The M06-2X[35] density-functional method in conjunction with the 6-311G(d,p) basis set was selected for all the geometry optimizations and frequency analysis. For reactions in solution phase, the geometries were optimized including solvation effects. For this purpose, the SMD solvation method was employed. Frequency calculations at 298.15 K on all the stationary points were carried out at the same level of theory as the geometry optimizations to ascertain the nature of the stationary points. Ground and transition states were characterized by none and one imaginary frequency, respectively. Additionally, intrinsic reaction coordinate (IRC) calculations were carried out on some transition states to ensure that they connect the corresponding intermediates. All of the presented relative energies are free energies at 298.15 K with respect to the reactants, unless otherwise stated.

General Remarks. ^{1}H NMR spectra were recorded on a 300 MHz instrument. ^{13}C NMR spectra were recorded on the same instrument at 75 MHz. Chemical shifts (δ) are expressed in parts per million downfield from TMS as an internal standard. The letters s, d, t, q, and m are used to indicate singlet, doublet, triplet, quadruplet, and multiplet, respectively. Analytical HPLC analysis was carried out on a C18 reversed-phase (RP) analytical column (150 × 4.6 mm; particle size, 5 mm) at 25 °C using a mobile phase A (water/acetonitrile 90:10 (v/v) + 0.1% TFA) and B (MeCN + 0.1% TFA) at a flow rate of 1.5 mL min^{-1}. The following gradient was applied: linear increase from solution 30% B to 50% B in 8 min, linear increase from solution 50% B to 100% B in 5 min, and hold at 100% solution B for 3 min. HPLC yields were determined by peak area integration (at 215 nm) corrected for relative response factors measured from standard solutions of the pure compounds. HPLC samples were prepared by dilution of 50 μL of the reaction mixture in 2 mL of acetonitrile. Melting points were determined on a standard melting point apparatus in open capillaries. The purity of all synthesized compounds (>98%) was established by either HPLC at 215 nm and/or ^{1}H NMR spectroscopy. All anhydrous solvents (stored over molecular sieves) and chemicals were obtained from standard commercial vendors and were used without any further purification. Substrates **1a**,[26a] **2**,[41b] and **3**[58] were prepared according to the described procedures.

Differential Scanning Calorimetry. Differential scanning calorimetry data were obtained on a PerkinElmer Pyris I instrument with the Pyris DSC Software v 8.0.1.0196. The DSC plots were recorded between 50 and 400 °C, with a heating rate of 10 °C min^{-1}, using 1−2 mg of substrate contained in sealed aluminum crucibles (12 bar max pressure).

General Experimental Procedure for Batch Microwave Processing. Microwave heating experiments were carried out in a Monowave 300 (Anton Paar GmbH, Graz, Austria) in sealed Pyrex microwave process vials using standard procedures.[15] Reaction times refer to hold times at the set maximum temperature indicated, not to total irradiation times. The temperature was measured using an internal fiber-optic temperature sensor. When the desired hold time was reached, the vial was cooled to 50 °C using compressed air. HPLC yields were determined by peak area integration (at 215 nm) corrected for relative response factors. Details for individual isolation procedures are collected in the Supporting Information.

General Experimental Procedure for Flow Processing. Flow experiments were performed using an X-Cube Flash instrument (ThalesNano Inc., Budapest, Hungary) equipped with a 4 mL stainless steel coil. The reaction parameters (temperature, flow rate, and pressure) were selected on the flow reactor, and the processing was started, whereby only pure solvent was pumped through the system until the instrument had achieved the desired reaction parameters and stable processing was assured. The inlet tube was then switched to the vial containing a freshly prepared solution of the corresponding substrate. A more detailed general description using this instrument has been published previously.[14]

2,2-Dimethyl-6-phenyl-1,3-dioxin-4-one (6a) (Scheme 1). 5-Benzoyl-2,2-dimethyl-1,3-dioxane-4,6-dione (**1a**) (124.1 mg, 0.5 mmol) was dissolved in dry DME (2 mL) under an argon atmosphere and subjected to pyrolysis under continuous-flow conditions (100 °C, 2 min residence time, 2 mL min^{-1} flow rate in a 4 mL stainless steel coil). The collected reaction mixture was evaporated under vacuum, and the crude mixture was purified by silica gel flash chromatography (hexane/ethyl acetate, gradient elution from 3:1 to 1:3) to obtain product **6a** (67 mg, 65%) as a colorless solid: mp 62−63 °C (lit.[59] mp 62−63 °C); ^{1}H NMR ($CDCl_3$) δ 7.72 (d, J = 8.14 Hz, 2H), 7.44−7.54 (m, 3H), 5.91 (s, 1H), 1.82 (s, 6H).

3-Benzoyl-6-phenyl-pyran-2,4-dione (7a) (Scheme 1). 5-Benzoyl-2,2-dimethyl-1,3-dioxane-4,6-dione (**1a**) (124.1 mg, 0.5 mmol) was dissolved in dry DME (2 mL) under an argon atmosphere and subjected to pyrolysis under continuous-flow conditions (200 °C, 1 min residence time, 4 mL min^{-1} flow rate in a 4 mL stainless steel coil). The collected reaction mixture was evaporated under vacuum, and the crude mixture was purified by silica gel flash chromatography (hexane/ethyl acetate, gradient elution from 3:1 to 1:3) to provide product **7a** (58 mg, 80%) as a yellowish solid: mp 172−173 °C (lit.[60] mp 169−170 °C); ^{1}H NMR ($CDCl_3$) δ 15.97 (s, 1H), 7.93 (d, J = 7.7 Hz, 1H), 7.71 (d, J = 7.9 Hz, 1H), 7.45−7.59 (m, 6H), 6.68 (s, 3H).

2-Phenyl-6*H*-1,3-oxazin-6-one (9) (Scheme 2). 5-*N*-(Benzamido)methylene-2,2-dimethyl-1,3-dioxane-4,6-dione (**2**) (137.6 mg, 0.5 mmol) was dissolved in dry toluene (2 mL) under an argon atmosphere and subjected to pyrolysis under continuous-flow conditions (270 °C, 30 s residence time, 8 mL min^{-1} flow rate in a 4 mL stainless steel coil). The collected reaction mixture was evaporated under vacuum, and the crude product was crystallized from hexane/toluene to provide oxazine **9** (76 mg, 88%) as a colorless solid: mp 82−83 °C (lit.[41b] mp 83−85 °C); ^{1}H NMR (DMSO-d_6) δ 8.12 (d, J = 7.9 Hz, 2H), 8.00 (d, J = 6.8 Hz, 1H), 7.69 (t, J = 7.4 Hz, 1H), 7.59 (t, J = 7.8 Hz, 2H), 6.42 (d, J = 6.8 Hz, 1H).

3-Methyl-2-phenylquinolin-4(1*H*)-one (11) (Scheme 3). A solution of pyrroledione **3** (52.6 mg, 0.2 mmol) in acetonitrile (2 mL) was pumped through the flow reactor (340 °C, 15 s residence time, 16 mL min^{-1} flow rate in a 4 mL stainless steel coil). The collected reaction mixture was evaporated under vacuum to provide quinolone **11** (47 mg, 99%) as colorless crystals: mp 284−285 (lit.[16] mp 283−285 °C); ^{1}H NMR (DMSO-d_6) δ 11.61 (s, 1H), 8.13 (d, J = 8.04 Hz, 1H), 7.58 (m, 6H), 7.30 (m, 1H), 1.89 (s, 3H).

Dipyrrolo[1,2-*a*:1',2'-*d*]pyrazine-5,10-dione (14) (Scheme 4). Methyl pyrrole-2-carboxylate (**4**) (25 mg, 0.2 mmol) was dissolved in acetonitrile (2 mL) and subjected to pyrolysis under continuous-flow conditions (330 °C, 7 min residence time, 0.6 mL min^{-1} flow rate in a 4 mL stainless steel coil). The collected reaction mixture was evaporated under vacuum. The resulting crystals were collected by filtration and washed with cold acetonitrile to provide 11 mg (55%) of product **14** as a yellow solid: mp 273−274 °C (lit.[49] mp 272−273 °C); ^{1}H NMR (CD_3Cl) δ 7.77 (dd, J = 3.00 Hz, J = 1.49 Hz, 1H), 7.40 (dd, J = 3.60 Hz, J = 1.42 Hz, 1H), 6.50 (t, J = 3.39 Hz, 1H).

ASSOCIATED CONTENT

Supporting Information

Supplementary tables and figures; copies of ^{1}H NMR spectra; detailed comments on the solvent expansion phenomena and azulene-to-naphthalene rearrangement calculations; complete ref 36; and Cartesian coordinates, energy, and imaginary frequency (transition states) for all the calculated stationary points. This material is available free of charge via the Internet at http://pubs.acs.org.

AUTHOR INFORMATION

Corresponding Author

*E-mail: oliver.kappe@uni-graz.at.

Present Address

[†]Department of Chemistry, Shahid Bahonar University of Kerman, Kerman 76169, Iran.

Notes

The authors declare no competing financial interest.

■ ACKNOWLEDGMENTS

This work was supported by a grant from the Christian Doppler Research Society (CDG). D.C. thanks the Spanish Ministerio de Ciencia e Innovación for a fellowship and the Research, Technological Innovation, and Supercomputing Center of Extremadura (CénitS) for their support in the use of LUSITANIA computer resources.

■ REFERENCES

(1) Brown, R. F. C. *Pyrolytic Methods in Organic Chemistry*; Academic Press: New York, 1980.

(2) (a) Seybold, G. *Angew. Chem., Int. Ed.* **1977**, *16*, 365−373. (b) Karpf, M. *Angew. Chem., Int. Ed.* **1986**, *25*, 414−430.

(3) (a) Wiersum, U. E. *Aldrichimica Acta* **1984**, *17*, 31−40. (b) McNab, H. *Aldrichimica Acta* **2004**, *37*, 19−26.

(4) For some recent examples on matrix isolation spectroscopy in combination with FVP, see: (a) Sander, W.; Exner, M.; Winkler, M.; Balster, A.; Hjerpe, A.; Kraka, E.; Cremer, D. *J. Am. Chem. Soc.* **2002**, *124*, 13072−13079. (b) Maier, G.; Reisenauer, H. P.; Glatthaar, J.; Zetzmann, R. *Chem.—Asian J.* **2006**, *1*, 195−202. (c) Wang, J.; Burdzinski, G.; Zhu, Z.; Platz, M. S.; Carra, C.; Bally, T. *J. Am. Chem. Soc.* **2007**, *129*, 8380−8388. (d) Neuhaus, P.; Grote, D.; Sander, W. *J. Am. Chem. Soc.* **2008**, *130*, 2993−3000. (e) Nunes, C. M.; Reva, I.; Pinho e Melo, T. M. V. D.; Fausto, R.; Šolomek, T.; Bally, T. *J. Am. Chem. Soc.* **2011**, *133*, 18911−18923. (f) Gerbig, D.; Reisenauer, H. P.; Wu, C.-H.; Ley, D.; Allen, W. D.; Schreiner, P. R. *J. Am. Chem. Soc.* **2010**, *132*, 7273.

(5) For an example of intermolecular FVP chemistry and a critical discussion of experimental variables in FVP, see: Duffy, E. F.; Foot, J. S.; McNab, H.; Milligan, A. A. *Org. Biomol. Chem.* **2004**, *2*, 2677−2683.

(6) There are several variations of FVP that do allow processing of nonvolatile substrates. See, for example, the following reference on solution-spray FVP: (a) Rubin, Y.; Lin, S. S.; Knobler, C. B.; Anthony, J.; Boldi, A. M.; Diederich, F. *J. Am. Chem. Soc.* **1991**, *113*, 6943. and piptopyrolysis (pipto = to fall): (b) Wentrup, C.; Mayor, C.; Becker, J.; Lindner, H.-J. *Tetrahedron* **1985**, *41*, 1601−1612.

(7) For a literature summary with over 300 references for 2011, see: (a) Glasnov, T. N. *J. Flow Chem.* **2011**, *1*, 46−51. (b) Glasnov, T. N. *J. Flow Chem.* **2011**, *1*, 90−96. (c) Glasnov, T. N. *J. Flow Chem.* **2012**, *2*, 28−36.

(8) For recent selected reviews on continuous-flow/microreactor chemistry, see: (a) Wiles, C.; Watts, P. *Green Chem.* **2012**, *14*, 38−54. (b) Noël, T.; Buchwald, S. L. *Chem. Soc. Rev.* **2011**, *40*, 5010−5029. (c) Baumann, M.; Baxendale, I. R.; Ley, S. V. *Mol. Diversity* **2011**, *15*, 613−630. (d) Hartman, R. L.; McMullen, J. P.; Jensen, K. F. *Angew. Chem., Int. Ed.* **2011**, *50*, 7502−7519. (e) Wiles, C.; Watts, P. *Chem. Commun.* **2011**, *47*, 6512−6535. (f) Wagner, J.; Ceylan, S.; Kirschning, A. *Chem. Commun.* **2011**, *47*, 4583−4592. (g) Yoshida, J.-i.; Kim, H.; Nagaki, A. *ChemSusChem* **2011**, *4*, 331−340. (h) McMullen, J. P.; Jensen, K. F. *Annu. Rev. Anal. Chem.* **2010**, *3*, 19−42. (i) Illg, T.; Löb, P.; Hessel, V. *Bioorg. Med. Chem.* **2010**, *18*, 3707−3719. (j) Geyer, K.; Gustafsson, T.; Seeberger, P. H. *Synlett* **2009**, 2382−2391.

(9) (a) Willes, C.; Watts, P. *Micro Reaction Technology in Organic Synthesis*; CRC Press: Boca Raton, FL, 2011. (b) Luis, S. V., Garcia-Verduqo, E., Eds. *Chemical Reactions and Processes under Flow Conditions*; Royal Society of Chemistry: Cambridge, U.K., 2010. (c) Wirth, T., Ed. *Microreactors in Organic Synthesis and Catalysis*; Wiley-VCH: Weinheim, Germany, 2008. (d) Hessel, V., Schouten, J. C., Renken, A., Wang, Y., Yoshida, J.-i., Eds. *Handbook of Micro Reactors*; Wiley-VCH: Weinheim, Germany, 2009. (e) Yoshida, J.-i. *Flash Chemistry: Fast Organic Synthesis in Microsystems*; Wiley-VCH: Weinheim, Germany, 2008.

(10) Razzaq, T.; Kappe, C. O. *Chem.—Asian J.* **2010**, *5*, 1274−1289 and references cited therein.

(11) Kappe, C. O.; Dallinger, D.; Murphree, S. S. *Practical Microwave Synthesis for Organic Chemists: Strategies, Instruments, and Protocols*; Wiley-VCH: Weinheim, Germany, 2009.

(12) (a) Jessop, P. G., Leitner, W., Eds. *Chemical Synthesis Using Supercritical Fluids*; Wiley-VCH: Weinheim, Germany, 1999. (b) van Eldik, R., Klärner, G., Eds. *High Pressure Chemistry: Synthetic, Mechanistic and Supercritical Applications*; Wiley-VCH: Weinheim, Germany, 2002. (c) Arai, Y.; Sako, T.; Takebayashi, Y. *Supercritical Fluids: Molecular Interactions, Physical Properties, and New Applications*; Springer: Berlin, 2002. (d) Licence, P.; Poliakoff, M. In *New Methodologies and Techniques for a Sustainable Organic Chemistry*; Mordini, A., Faigl, F., Eds.; Springer: Dordrecht, 2008.

(13) (a) Yoon, C. S.; Park, H. D.; Kim, S. Y.; Kim, S. H. *Macromol. Symp.* **2007**, *249−250*, 515−520. (b) Choia, H.; Veriansyaha, B.; Kima, J.; Kima, J.-D.; Kang, J. W. *J. Supercrit. Fluids* **2010**, *52*, 285−291. (c) Tilstam, U.; Defrance, T.; Giard, T. *Org. Process Res. Dev.* **2009**, *13*, 312−323. (d) Nursanto, E. B.; Nugroho, A.; Hong, S.-A.; Kim, S. J.; Chung, K. Y.; Kim, J. *Green Chem.* **2011**, *13*, 2714−2718.

(14) For a detailed description of this reactor, see: Razzaq, T.; Glasnov, T. N.; Kappe, C. O. *Chem. Eng. Technol.* **2009**, *32*, 1702−1716.

(15) (a) Obermayer, D.; Gutmann, B.; Kappe, C. O. *Angew. Chem., Int. Ed.* **2009**, *48*, 8321−8342. (b) Obermayer, D.; Kappe, C. O. *Org. Biomol. Chem.* **2010**, *8*, 114−121.

(16) Lecoq, D.; Chalmers, B. A.; Veedu, R. N.; Kvaskoff, D. K.; Bernhardt, P. V.; Wentrup, C. *Aust. J. Chem.* **2009**, *62*, 1631−1638.

(17) Gudipati, I. R.; Sadasivam, D. V.; Birney, D. M. *Green Chem.* **2008**, *10*, 275−277.

(18) Cho, H. Y.; Ajaz, A.; Himali, D.; Waske, P. A.; Johnson, R. P. *J. Org. Chem.* **2009**, *74*, 4137−4142.

(19) For a recent review, see: Glasnov, T. N.; Kappe, C. O. *Chem.—Eur. J.* **2011**, *17*, 11956−11968 and references cited therein.

(20) Tidwell, T. T. *Ketenes*, 2nd ed.; John Wiley & Sons: New York, 2006.

(21) (a) Hyatt, J. A.; Reynolds, P. W. *Org. React.* **1994**, *45*, 159−646. (b) Moore, H. W.; Decker, O. H. W. *Chem. Rev.* **1986**, *86*, 821−830.

(22) Höhne, G.; Hemminger, W.; Flammersheim, H.-J. *Differential Scanning Calorimetry*; Springer-Verlag: Berlin, 2003.

(23) For applications of DSC in synthetic organic chemistry, see: (a) Review: Kappe, T.; Stadlbauer, W. *Molecules* **1996**, *1*, 255−263. (b) Butenschön, H. *Chem. Ber.* **1993**, *126*, 1651−1656. (c) Butenschön, H. *Chem. Ber.* **1994**, *127*, 137−144. (d) Bollinger, F.; Tuma, L. D. *Synlett* **1996**, 407−420. (e) Hagan, D. J.; Gimenez-Arnau, E.; Schwalbe, C. H.; Stevens, M. F. G. *J. Chem. Soc., Perkin Trans. 1* **1997**, 2739−2746. (f) Stadlbauer, W.; Fiala, W.; Fischer, M.; Hojas, G. *J. Heterocycl. Chem.* **2000**, *37*, 1253−1256. (g) Hojas, G.; Fiala, W.; Stadlbauer, W. *J. Heterocycl. Chem.* **2000**, *37*, 1559−1569.

(24) For a review, see: Gaber, A. M.; McNab, H. *Synthesis* **2001**, 2059−2074.

(25) For a review on the chemistry of α-oxoketenes, see: Wentrup, C.; Heilmayer, W.; Kollenz, G. *Synthesis* **1994**, 1219−1248.

(26) (a) Yamamoto, Y.; Watanabe, Y.; Ohnishi, S. *Chem. Pharm. Bull.* **1987**, *35*, 1860−1870. (b) Emtenäs, H.; Alderin, L.; Almqvist, F. *J. Org. Chem.* **2001**, *66*, 6756−6761. (c) Emtenäs, H.; Soto, G.; Hultgren, S. J.; Marshall, G. R.; Almqvist, F. *Org. Lett.* **2000**, *2*, 2065−2067. (d) Pemberton, N.; Jakobsson, L.; Almqvist, F. *Org. Lett.* **2006**, *8*, 935−938.

(27) Shumway, W.; Ham, S.; Moer, J.; Whittlesey, B. R.; Birney, D. M. *J. Org. Chem.* **2000**, *65*, 7731−7739.

(28) Morita, Y.; Kamakura, R.; Takeda, M.; Yamamoto, Y. *Chem. Commun.* **1997**, 359−360.

(29) Oikawa, Y.; Sugano, K.; Yonemitsu, O. *J. Org. Chem.* **1978**, *43*, 2087−2088.

(30) Yamamoto, Y.; Ohnishi, S.; Azuma, Y. *Chem. Pharm. Bull.* **1982**, *30*, 3505−3512.

(31) (a) Kappe, C. O.; Wong, M. W.; Wentrup, C. *J. Org. Chem.* **1995**, *60*, 1686−1695. (b) Zuhse, R. H.; Wong, M. W.; Wentrup, C. *J. Phys. Chem.* **1996**, *100*, 3917−3922.
(32) (a) Hyatt, J. A.; Feldman, P. L.; Clemens, R. J. *J. Org. Chem.* **1984**, *49*, 5105−5108. (b) Clemens, R. J.; Hyatt, J. A. *J. Org. Chem.* **1984**, *50*, 2431−2435. (c) Sato, M.; Ogasawara, H.; Komatsu, S.; Kato, T. *Chem. Pharm. Bull.* **1984**, *32*, 3848−3856.
(33) (a) Freiermuth, B.; Wentrup, C. *J. Org. Chem.* **1991**, *56*, 2286−2289. (b) Gammill, R. B.; Judge, T. M.; Phillips, G.; Zhang, Q.; Sowell, C. G.; Cheney, B. V.; Mizsak, S. A.; Dolak, L. A.; Seest, E. P. *J. Am. Chem. Soc.* **1994**, *116*, 12113−12114. (c) Birney, D. M.; Xu, X.; Ham, S.; Huang, X. *J. Org. Chem.* **1997**, *62*, 7114−7120.
(34) For the direct IR spectroscopic observation of benzoylketene, see: Andreichikov, Y. S.; Kollenz, G.; Kappe, C. O.; Leung-Toung, R.; Wentrup, C. *Acta Chem. Scand.* **1992**, *46*, 683−685.
(35) Zhao, Y.; Truhlar, D. G. *Theor. Chem. Acc.* **2008**, *120*, 215−241.
(36) Frisch, M. J.;et al. *Gaussian 09*, revision A.1; Gaussian, Inc.: Wallingford, CT, 2009.
(37) Marenich, A. V.; Cramer, C. J.; Truhlar, D. G. *J. Phys. Chem. B* **2009**, *113*, 6378−6396.
(38) Since DME is not included in the Gaussian internal solvent list, tetrahydrofuran was selected as solvent for the calculations because of the similar solvation properties.
(39) Damm, M.; Glasnov, T. N.; Kappe, C. O. *Org. Process Res. Dev.* **2010**, *14*, 215−224.
(40) For the flow experiments shown in Figure 4b, a 2.5 mL steel coil fitted to a Uniqsis FlowSyn reactor was used. See the following reference and the Supporting Information for further details: Gutmann, B.; Roduit, J.-P.; Roberge, D.; Kappe, C. O. *J. Flow Chem.* **2012**, *2*, 8−19.
(41) (a) Wentrup, C.; Finnerty, J. J.; Koch, R. *Curr. Org. Chem.* **2010**, *14*, 1586−1599. (b) McNab, H.; Withell, K. *Tetrahedron* **1996**, *52*, 3163−3170. (c) McNab, H.; Morrow, M.; Parsons, S.; Shannon, D. A.; Withell, K. *Org. Biomol. Chem.* **2009**, *7*, 4936−4942.
(42) Yamamoto, Y.; Morita, Y.; Minami, K. *Chem. Pharm. Bull.* **1986**, *34*, 1980−1986.
(43) For theoretical calculations on the formation of 1,3-oxazin-6-ones from *N*-acylimidoylketenes, see: (a) Alajarín, M.; Vidal, A.; Sánchez-Andrada, P.; Tovar, F.; Ochoa, G. *Org. Lett.* **2000**, *2*, 965−968. (b) Alajarín, M.; Sánchez-Andrada, P. *J. Org. Chem.* **2001**, *66*, 8470−8477. (c) Bornemann, H.; Wentrup, C. *J. Org. Chem.* **2005**, *70*, 5862−5868.
(44) (a) Kappe, C. O.; Kollenz, G.; Leung-Toung, R.; Wentrup, C. *J. Chem. Soc., Chem. Commun.* **1992**, 478−488. (b) Fulloon, B.; El-Nabi, H. A. A.; Kollenz, G.; Wentrup, C. *Tetrahedron Lett.* **1995**, *36*, 6547−6550. (c) Fulloon, B.; Wentrup, C. *J. Org. Chem.* **1996**, *61*, 1363−1368. (d) Ramana Rao, V. V.; Wentrup, C. *J. Chem. Soc., Perkin Trans. 1* **2002**, 1232−1235.
(45) The decomposition of pyrroledione **3** with concomitant gas release was visually observed in a sealed capillary tube at 310−320 °C. HPLC analysis of the resulting residue showed quinolone **11** as the only product of this solvent-free transformation.
(46) (a) Razzaq, T.; Kappe, C. O. *Eur. J. Org. Chem.* **2009**, 1321−1325. (b) Sedelmeier, J.; Ley, S. V.; Baxendale, I. R. *Green Chem.* **2009**, *11*, 683−685. (c) Glasnov, T.; Findenig, S.; Kappe, C. O. *Chem.—Eur. J.* **2009**, *15*, 1001−1010. (d) Obermayer, D.; Glasnov, T. N.; Kappe, C. O. *J. Org. Chem.* **2011**, *76*, 6657−6669.
(47) It should be noted that, at these high temperatures, the importance of solvent expansion phenomena on the determination of the factual residence times cannot be neglected. See the Supporting Information (Figure S4) and the following references for more details: (a) Martin, R. E.; Morawitz, F.; Kuratli, C.; Alker, A. M.; Alanine, A. I. *Eur. J. Org. Chem.* **2012**, 47−52. (b) See also ref 13c.
(48) George, L.; Netsch, K.-P.; Penn, G.; Kollenz, G.; Wentrup, C. *Org. Biomol. Chem.* **2006**, *4*, 558−564.
(49) Qiao, G. G.; Meutermans, W.; Wong, M. W.; Träubel, M.; Wentrup, C. *J. Am. Chem. Soc.* **1996**, *118*, 3852−3861 and references cited therein.
(50) The formation of 2,5-diketopiperazines from amino acids is typically only possible in the presence of activating reagents or catalysts; see: (a) Jainta, M.; Nieger, M.; Bräse, S. *Eur. J. Org. Chem.* **2008**, 5418−5424. (b) Ciamician, G. L.; Silber, P. *Chem. Ber.* **1884**, *17*, 103−106. (c) Bidasee, K. R.; Nallani, K.; Besch, H. R. Jr.; Dincer, U. D. *J. Pharmacol. Exp. Ther.* **2003**, *305*, 989−998. (d) Nonappa; Ahonen, K.; Lahtinen, M.; Kolehmainen, E. *Green Chem.* **2011**, *13*, 1203−1209.
(51) (a) Krapcho, A. P.; Weimaster, J. F.; Eldridge, J. M.; Jahngen, E. G. E.; Lovey, A. J.; Stephens, W. P. *J. Org. Chem.* **1978**, *43*, 138−147. (b) Krapcho, A. *Tetrahedron Lett.* **1974**, *15*, 1091−1094. (c) Krapcho, A. *Tetrahedron Lett.* **1967**, *8*, 215−217.
(52) (a) Heilbronner, E.; Plattner, P. A.; Wieland, K. *Experientia* **1947**, *3*, 70−71. (b) Heilbronner, E.; Wieland, K. *Helv. Chim. Acta* **1947**, *30*, 947−956.
(53) (a) Alder, R. W.; Whittaker, G. *J. Chem. Soc., Perkin Trans. 2* **1975**, 714−723. (b) Alder, R. W.; Wilshire, C. *J. Chem. Soc., Perkin Trans. 2* **1975**, 1464−1468. (c) Alder, R. W.; Whiteside, R. W.; Whittaker, G.; Wilshire, C. *J. Am. Chem. Soc.* **1979**, *101*, 629−632. (d) Becker, J.; Wentrup, C.; Katz, E.; Zeller, K. P. *J. Am. Chem. Soc.* **1980**, *102*, 5110−5112. (e) Zeller, K. P.; Wentrup, C. *Z. Naturforsch.* **1981**, *36B*, 852−857. (f) Scott, L. T. *Acc. Chem. Res.* **1982**, *15*, 52−58. (g) Gugel, H.; Zeller, K.-P.; Wentrup, C. *Chem. Ber.* **1983**, *116*, 2775−2784.
(54) (a) Dewar, M. J. S.; Merz, K. M. *J. Am. Chem. Soc.* **1985**, *107*, 6111−6114. (b) Dewar, M. J. S.; Merz, K. M. *J. Am. Chem. Soc.* **1986**, *108*, 5142−5145. (c) Dewar, M. J. S.; Merz, K. M. *J. Am. Chem. Soc.* **1986**, *108*, 5146−5153.
(55) Alder, R. W.; East, S. P.; Harvey, J. N.; Oakley, M. T. *J. Am. Chem. Soc.* **2003**, *125*, 5375−5387.
(56) Stirling, A.; Iannuzzi, M.; Laio, A.; Parrinello, M. *ChemPhysChem* **2004**, *5*, 1558−1568.
(57) Recent evidence suggests that this rearrangement can also be performed using a technique referred to as "microwave flash pyrolysis" whereby azulene is mixed with a strong microwave-absorbing substance (e.g., graphite) and is subsequently irradiated with microwaves. The superheating of the support to extreme temperatures will then trigger the thermal isomerization. See ref 18 for details.
(58) Cobas, A.; Guitian, E.; Castedo, L. *J. Org. Chem.* **1993**, *58*, 3113−3117.
(59) Sato, M.; Ogasawara, H.; Oi, K.; Kato, T. *Chem. Pharm. Bull.* **1983**, *31*, 1896−1901.
(60) Akbas, E.; Sonmez, M.; Anil, B.; Aslanoglu, F. *Russ. J. Gen. Chem.* **2008**, *78*, 1277−1282.